Journal of Building Engineering 119 (2026) 115308

Contents lists available at ScienceDirect

Journal of Building Engineering

journal homepage: www.elsevier.com/locate/jobe

# Toward low-carbon 3D concrete printing through circular construction and waste valorization

Xiaoshao Mu [a,b], Xiaoling Zhang [c,d,*], Gang He [e], K.M. Liew [a,b,**]

[a] Department of Architecture and Civil Engineering, City University of Hong Kong, Kowloon, Hong Kong Special Administrative Region of China
[b] Centre for Nature-Inspired Engineering, City University of Hong Kong, Kowloon, Hong Kong Special Administrative Region of China
[c] Department of Real Estate and Construction, Faculty of Architecture, The University of Hong Kong, Pokfulam, Hong Kong Special Administrative Region of China
[d] Sustainability X-Lab, Faculty of Architecture, The University of Hong Kong, Pokfulam, Hong Kong Special Administrative Region of China
[e] Marxe School of Public and International Affairs, Baruch College, City University of New York, New York, 10010, USA

ARTICLE INFO

*Keywords:*
Life cycle assessment
3D concrete printing
Recycled materials
Waste valorization
Sustainability

ABSTRACT

The construction industry's intensive resource consumption and significant carbon footprint underscore the urgent need for transformative technologies to achieve global sustainability goals. This study conducts a comprehensive cradle-to-grave life cycle assessment (LCA) to compare three-dimensional concrete printing (3DCP) with conventional construction, explicitly integrating waste reuse within a circular economy framework. Six construction scenarios are evaluated using the LCA methodology combined with a novel waste offset model, quantifying environmental impacts across 18 midpoint and 3 endpoint indicators. Monte Carlo simulations are employed to validate the robustness of the results. Findings reveal that the environmental advantages of 3DCP are conditional—substantial benefits emerge only when recycled materials and process optimizations are incorporated. Optimized 3DCP reduces life cycle carbon emissions by up to 53.1 %, while the use of recycled materials offsets as much as 21.8 % of process-related $CO_2$ emissions, aligning with the Global Cement and Concrete Association (GCCA) decarbonization targets. Concrete carbonation during use further cuts 3.92–7.69 % of total carbon footprint. Key constraints affecting 3DCP sustainability include high cement content, transportation energy demand, and dependency on chemical admixtures. The study highlights targeted material optimization, energy-efficient process design, and supportive policy measures as critical pathways for advancing 3DCP toward net-zero construction, thereby providing theoretical support for the construction, 3D printing, and environmental protection industries.

## 1. Introduction

Concrete is integral to global infrastructure, prized for its durability, mechanical properties, and workability [1]. However, its production and use present significant sustainability challenges across environmental, economic, and social dimensions. The construction sector is a major consumer of natural resources and a generator of waste throughout the building life cycle, substantially

* Corresponding author.
** Corresponding author. Department of Architecture and Civil Engineering, City University of Hong Kong, Kowloon, Hong Kong Special Administrative Region of China.
*E-mail addresses:* zhangxl@hku.hk (X. Zhang), kmliew@cityu.edu.hk (K.M. Liew).

https://doi.org/10.1016/j.jobe.2026.115308
Received 10 October 2025; Received in revised form 28 December 2025; Accepted 13 January 2026
Available online 13 January 2026
2352-7102/

contributing to global greenhouse gas emissions and adversely impacting local ecosystems [2]. Economically, the industry is characterized by high costs driven by intensive labor requirements and expensive construction and maintenance processes [3]. Socially, hazardous production and construction environments pose substantial risks to worker health and safety [4].

Consequently, there is an urgent need to develop sustainable construction technologies that decouple development from environmental degradation. These technologies are essential to reduce the extraction of virgin resources, minimize waste generation, lower greenhouse gas emissions, and enhance building longevity [5]. Within this context, 3DCP has emerged as a transformative solution. 3DCP offers the potential to revolutionize construction practices by diminishing material waste, curbing energy consumption, and slashing carbon emissions. Furthermore, it can lower costs through automation, improve structural safety, and create new opportunities to address housing affordability and social sustainability [6,7].

However, the widespread adoption of 3DCP faces several interconnected barriers. A primary challenge lies in material development, as novel compositions must satisfy stringent requirements for printability, structural strength, long-term durability, and sustainability [8–10]. Concurrently, technological advancements are needed to improve printing speed, resolution, and reliability to meet the demands of large-scale projects [11]. The inherent complexity of 3DCP also demands a fundamental shift in architectural design principles and the establishment of new standards to ensure structural integrity and safety [12]. Furthermore, life cycle management introduces unique challenges, necessitating innovative strategies for the maintenance, repair, and end-of-life recycling of printed structures. To achieve true disruption, 3DCP must become cost-competitive through reductions in equipment and material expenses [13]. Finally, a comprehensive assessment of its environmental footprint—encompassing energy consumption, emissions, and resource use—is essential to verify its alignment with sustainability goals and regulatory frameworks [14]. Overcoming these multifaceted barriers will require coordinated innovation across material science, engineering, design, and policy to fully unlock the transformative potential of 3DCP.

The integration of waste streams as supplementary cementitious materials (SCMs) offers a significant pathway to improve the sustainability of 3DCP [15]. This approach addresses a pressing environmental challenge: the construction sector accounts for approximately 40 % of global solid waste, 40 % of material consumption, and 33 % of carbon emissions [16]. In this context, 3DCP serves as a key technical enabler of circular economy principles, which seek to decouple economic growth from resource depletion by closing material loops [17]. The unique process constraints and material requirements of 3DCP can further drive the valorization of diverse waste streams, converting them from landfill burdens into valuable construction resources.

Research demonstrates that diverse industrial by-products and post-consumer wastes, including rubber, polymers, construction and demolition waste, and recycled glass, can be effectively incorporated into 3DCP mixes [18–20]. These materials not only function as alternatives to virgin binders and aggregates, thereby reducing cement consumption and its associated carbon footprint [21], but can also enhance the material's fresh and hardened properties. Studies indicate that 3DCP mixes incorporating waste SCMs can attain extrudability, buildability, mechanical properties, and durability levels either comparable to or even superior to those of conventional cement-based mixes [22–24]. Moreover, specific waste materials have been engineered to address key 3DCP challenges. For instance, agricultural waste has been used to improve internal curing, microstructure, and interlayer bonding while reducing shrinkage [25,26]. The synergy between waste valorization and 3DCP thus provides a multi-faceted pathway toward more sustainable construction, reducing dependency on primary materials, minimizing waste disposal, and lowering the embodied carbon of structures, while simultaneously maintaining or improving technical performance. Realizing this circular potential demands continued innovation in material formulation and a systemic approach to integrating supply chains across industrial sectors.

Building upon this foundation, our research establishes a comprehensive framework for integrating waste streams into the 3DCP supply chain from a full life cycle perspective, with a specific focus on developing a waste reuse offset model. While prior studies have often assessed the substitution potential of individual waste materials in isolation, they generally lack a systemic mechanism to quantify the cascading environmental benefits of such reuse. Our work bridges this gap by introducing a multidimensional integration analysis that quantifies pollution avoidance and emission reduction effects—such as reduced landfilling energy demand and diminished pollution flows into natural systems—achieved through systematic offset mechanisms. By calculating these benefits across the entire life cycle, from raw material extraction to end-of-life disposal, this framework offers implementable strategies for scaling sustainable 3DCP and provides robust theoretical and practical guidance for maximizing resource efficiency in the built environment.

## 2. Research materials and methods

### 2.1. Life cycle assessment

This study conducted a LCA in accordance with ISO 14040 [27] and ISO 14044 [28] standards. The LCA framework comprised four phases: (1) goal and scope definition, (2) life cycle inventory (LCI) analysis, (3) life cycle impact assessment (LCIA), and (4) interpretation. Inventory modeling and impact assessment were executed using SimaPro software (version 10.1) in conjunction with the Ecoinvent database (version 3.10, cut-off system model).

#### 2.1.1. Goal and scope definition

The goal of this LCA is to compare the environmental impacts of 3DCP and conventional construction methods and to identify key contributors to these impacts, thereby informing targeted sustainability strategies. A primary pathway for mitigating the environmental footprint of concrete involves the large-scale integration of waste streams as resources [29]. Although industrial byproducts such as fly ash and silica fume are well-established SCMs, this study specifically assesses the effectiveness and potential of five novel or underutilized waste materials within 3DCP applications.

As shown in Fig. 1, Scenario 1 (S1) serves as the baseline for conventional construction technique. Scenarios 2 to 6 (S2–S6) were selected to evaluate the environmental performance of 3DCP incorporating the various waste materials recognized from literature as viable alternative materials. A cradle-to-grave system boundary is defined, encompassing raw material extraction and processing, material transportation, construction, use phase, and end-of-life management. The use phase is restricted to carbonation uptake and excludes operational energy consumption, which is assumed to be identical across all scenarios owing to the same building geometry and functional requirements. Waste-derived materials incorporated in the 3DCP scenarios are modeled using a cut-off allocation approach, whereby upstream environmental burdens associated with waste generation are excluded, and credits are assigned only for the avoided impacts of conventional waste treatment. The detailed assumptions and calculation procedures for waste offset modeling are provided in the following section.

A residential building with a height of 13.5 m was adopted as the functional unit for this study. This scale corresponds to the current applicable height range of 3D printing construction technology and reflects typical low-rise civil buildings in China. Design parameters and construction data were sourced from an actual project, utilizing domestic material supply chains and complying with regional industry standards. This approach enhances the practical relevance of the assessment and ensures alignment with local industrial practices and market conditions. The building geometry, spatial layout, and intended use are kept identical across all scenarios to ensure a consistent basis for comparison. The functional unit represents a typical low-rise residential building, a construction typology for which both conventional cast-in-place concrete and 3D-printed concrete systems have been increasingly investigated and applied. Specific building details are provided in Fig. 2.

The analysis assumes a 50-year service life for the structure, consistent with standard building lifespans. This temporal boundary is integral to the cradle-to-grave assessment, encompassing long-term environmental impacts from material production, construction, operation, and end-of-life disposal. This assumption is adopted solely as a baseline for comparative assessment and does not imply a prediction of actual durability performance; its implications are further discussed as a source of uncertainty in Section 4.2. This research framework is not limited to a single country or specific case study, instead, it is generalizable and can be applied to other case studies.

### 2.1.2. *Key assumptions and scenario equivalence*

Six construction scenarios are evaluated in this study. Scenario 1 represents a conventional reinforced concrete building constructed using formwork-based cast-in-place methods. Scenarios 2–6 represent alternative 3DCP pathways incorporating different waste-derived or recycled materials as partial replacements for cement and/or aggregates. The selected 3DCP mixtures are exclusively sourced from peer-reviewed studies in which material formulation, printability, and mechanical performance were experimentally investigated.

Equivalence among the construction scenarios is defined at the level of functional structural performance, rather than by assuming identical material behavior between conventionally cast concrete and additively manufactured concrete. Structural equivalence is therefore established in terms of the ability to deliver the same building function, rather than identical material-level mechanical

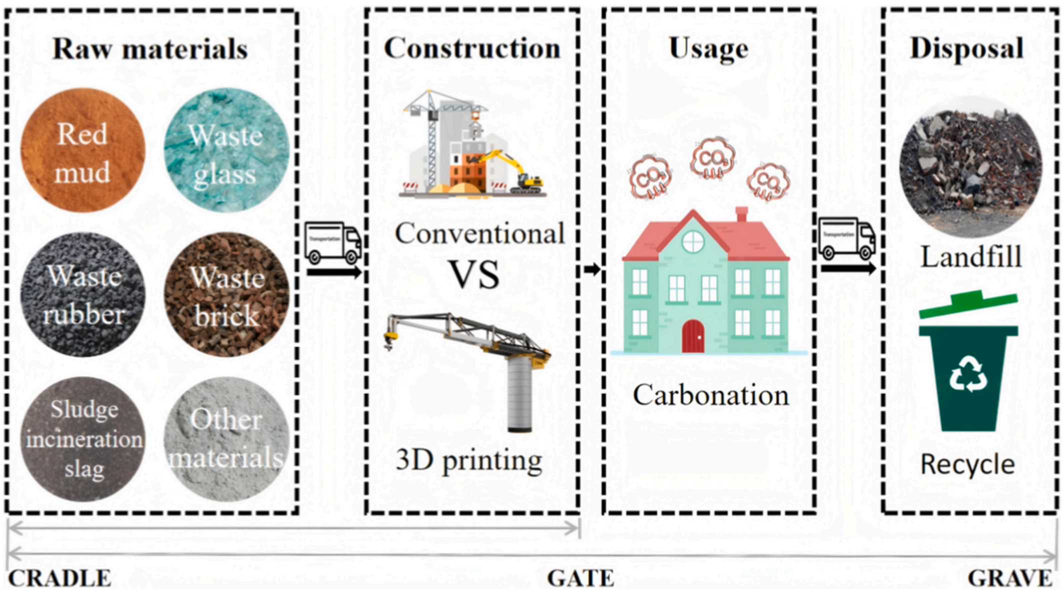


**Fig. 1.** The system boundary of the LCA model.
Note: Six scenarios were defined based on the manufacturing processes and material compositions: S1 (Baseline): Conventional cast-in-place concrete construction utilizing rebar, formwork, and ordinary Portland cement (OPC) concrete; S2: 3DCP utilizing a geopolymer binder derived from brick waste; S3: 3DCP incorporating waste glass; S4: 3DCP incorporating waste rubber; S5: 3DCP incorporating red mud; S6: 3DCP incorporating sludge incineration bottom ash.


**Fig. 2.** Schematic diagram of the residential building.

properties. The 3D printed concrete mixtures adopted in Scenarios 2–6 were selected from peer-reviewed literature reporting experimental validation of printability and mechanical performance, including compressive strength, interlayer bonding, and, where available, directional strength. Reported 28-day compressive strengths generally meet or exceed the requirements for low-rise load-bearing applications, supporting their suitability for structural use.

From an engineering design perspective, the anisotropic behavior of 3D printed concrete is typically treated as a design consideration rather than a prohibitive limitation. Previous studies have shown that layer-induced anisotropy can be mitigated through improvements in interlayer bonding, material and interface engineering, and anisotropy-aware structural detailing and print path planning [30–32]. In the present study, these established design considerations are implicitly accounted for through the definition of the functional unit and the selection of structurally validated 3DCP mixtures. Detailed anisotropy-aware structural design and optimization are therefore not explicitly modeled but are treated as prerequisites for functional equivalence, consistent with the scope of a comparative life cycle assessment. In practical applications, such functional equivalence would be ensured through compliance with applicable structural design codes and safety factors, which are assumed to be satisfied for all scenarios.

With respect to service life, a 50-year lifespan was adopted for all scenarios. This assumption is widely used in LCA studies on 3DCP [33–35] and aligns with typical building design lifetimes. While long-term durability data for some waste-incorporated 3DCP mixes are still evolving, applying a uniform service life ensures consistent cradle-to-grave comparisons and conforms to standard temporal boundaries in the field.

To clarify the comparative framework and enhance transparency, the core assumptions underlying the LCA are summarized in Table 1.

### 2.1.3. Waste offset model

Unlike conventional attributional LCA studies, in which waste management impacts are typically embedded within background datasets, the proposed waste offset model explicitly isolates the environmental implications of waste diversion through the introduction of a dedicated offset term. The net environmental impact is quantified by jointly accounting for the environmental burdens of primary raw material production and the avoided impacts of baseline waste treatment associated with the utilization of waste-derived materials, within a consistent cut-off system boundary.

This study explicitly quantifies the additional environmental benefits arising from the diversion of waste materials from landfill, effects that are typically embedded within background waste treatment datasets rather than isolated in conventional LCA frameworks. In the baseline scenario, waste-derived materials such as waste brick, waste glass, and other mineral wastes are assumed to be managed through regional sanitary landfill, representing a conservative and widely applied waste treatment pathway in the Chinese context. The environmental burdens associated with landfill disposal, including operational energy use and emissions as represented in ecoinvent waste treatment datasets, are therefore attributed to the waste-generating activities rather than to downstream material users. To achieve this, we clearly distinguish upstream from downstream burdens. In the Ecoinvent cut-off model, the upstream burden assigns the full environmental impact of producing a primary product solely to that product. Consequently, waste materials (e.g., waste brick, waste glass) that enter our system as recycled inputs carry zero or negligible upstream burdens in our life cycle inventory, thereby avoiding double-counting of their original production impacts.

It should be noted that the proposed waste offset model is implemented within an attributional LCA framework using a cut-off by classification approach. Although the offset term explicitly accounts for the effects of waste diversion, it does not represent system expansion, market-mediated substitution, or avoided emissions in a consequential sense. Instead, the offset reflects the avoided provision of waste treatment services that would otherwise be required under the baseline waste management pathway. This explicit accounting makes an effect visible that is often implicit within background datasets, while remaining fully consistent with attributional cut-off modeling principles.

The downstream burden offset, represented by the $P_{offset}$ term in our model, exclusively captures the environmental impacts associated with the avoided landfill disposal process for these waste materials had they not been utilized in 3DCP. This includes the avoidance of energy consumption and emissions from landfill operations, as well as the long-term emissions resulting from landfill leachate and decomposition. The avoided landfill burdens are calculated solely based on the corresponding ecoinvent waste treatment datasets, without introducing additional long-term emissions beyond those already accounted for in the database.

This method centers on the environmental value of waste reuse, establishing a distinct quantitative framework separate from conventional raw material substitution. The net impact is expressed as:

$$P = P_{materials} - P_{offset} + P_{manufacturing} + P_{use} + P_{disposal} + P_{transportation}. \quad (1)$$

$P_{materials}$ is the pollution generated during the raw material extraction and material production stages. $P_{offset}$ is the environmental burdens of landfill treatment activities that would otherwise be required for waste materials not reused in the system, including energy consumption and emissions associated with landfill operations, waste degradation, and leachate generation. $P_{manufacturing}$ is the energy consumption caused by equipment use during building construction stage. $P_{use}$ is the net environmental impact of carbonation during the concrete usage process. $P_{disposal}$ is the treatment of waste concrete. $P_{transportation}$ is the energy consumption and greenhouse gas emissions from vehicles transporting materials to construction sites and disposal sites during both production and scrapping. See the following section for specific calculations.

Fig. 3 presents the life cycle impact accounting framework of the proposed LCA model, encompassing material production, transportation, construction, use, end-of-life treatment, and the waste offset implemented under the cut-off approach. The figure emphasizes how avoided waste treatment services are explicitly accounted for alongside conventional life cycle impact components.

### 2.1.4. Life cycle inventory

The life cycle inventory data for conventional construction (S1) were obtained from an active real estate project developed by Central China Real Estate Group. Concrete and reinforced concrete data from this project were used to establish a baseline material inventory. Notably, the selection of this baseline is not only aligned with the currently implementable size of 3D printed buildings and their application proportion, but also corresponds to a prevalent characteristic of China's building stock [36,37]. The formwork inventory was derived directly from the bill of quantities of the reference real estate project, ensuring that the material types and

**Table 1**
Key assumptions underpinning the LCA framework.

| No. | Assumption | Description |
|---|---|---|
| 1 | Functional unit | A low-rise residential building (13.5 m height) providing equivalent structural function across all scenarios |
| 2 | Service life | A uniform service life of 50 years assumed for all scenarios |
| 3 | System boundary | Cradle-to-grave life cycle, including material production, construction, use phase, and end-of-life |
| 4 | Structural performance | 3D printed concrete is assumed to be structurally adequate for the intended building application |

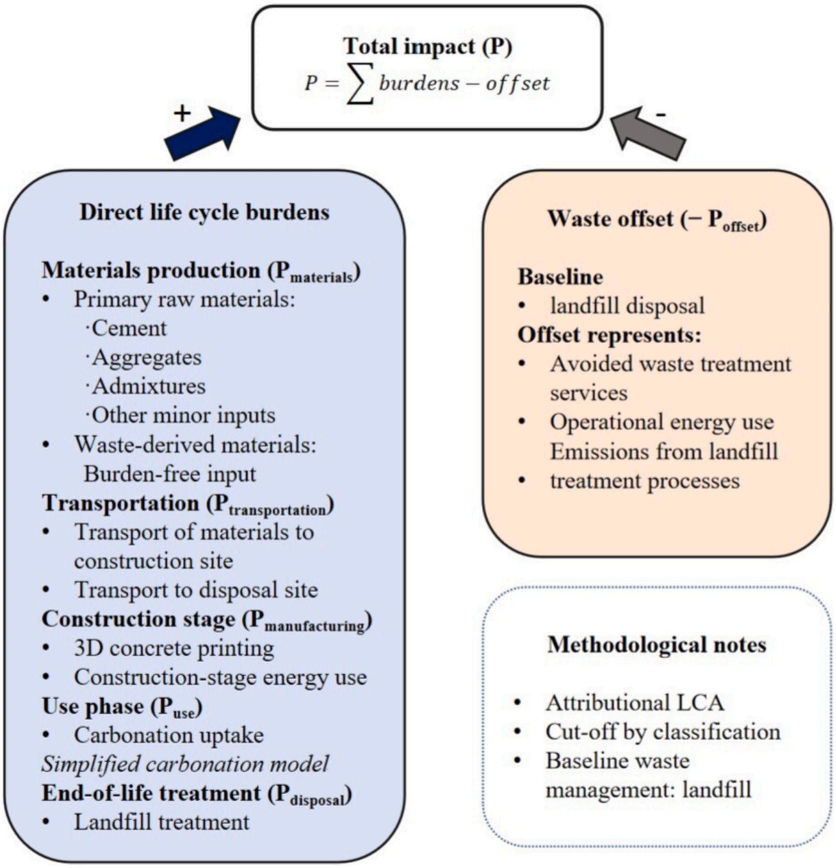


**Fig. 3.** LCA framework incorporating waste offset under a cut-off allocation approach.

quantities accurately reflect actual construction practice. To account for formwork reuse across multiple construction cycles, turnover frequencies and loss rates were determined in accordance with the local *National Unified Compilation Manual for Construction Engineering Basic Quotas* [38]. Consequently, the emissions attributed to the formwork system in scenario S1 incorporate a realistic, region-specific representation of material efficiency achieved through reuse.

For the 3DCP scenarios (S2–S6), material compositions were adopted from peer-reviewed literature (see Table 2 for detailed mix designs and corresponding references). All adopted mix designs were verified to meet the mechanical property requirements specified in concrete structure design standards. Complete life cycle inventory data for all six scenarios are provided in Tables 3 and 4.

#### *2.1.5. Impact assessment*

The LCIA was conducted using the ReCiPe 2016 method, a widely adopted framework for translating inventory data into environmental impact scores [43]. This method enables the characterization, normalization, and weighting of emissions and resource uses across multiple impact categories [44].

For this analysis, we employed the hierarchist (H) perspective with average weighting, as it reflects the prevailing scientific

**Table 2**
Mixed proportions for 3D printing concrete scenarios (unit: kg/m$^3$).

| Waste type | Scenario 2 [39] | Scenario 3 [40] | Scenario 4 [41] | Scenario 5 [42] | Scenario 6 [24] |
|---|---|---|---|---|---|
| | Waste brick | Red mud | Waste rubber | Waste glass | Sludge incineration slag |
| **Recycled materials** | 68.46 | 110 | 33.76 | 200 | 319.18 |
| **Cement** | – | 320 | 511.44 | 800 | 1276.71 |
| **Sand** | 1026.87 | 645 | 358.01 | 1000 | 957.53 |
| **Granite** | – | 870 | – | – | – |
| **Water** | 273.83 | 195 | 332.44 | 350 | 478.77 |
| **Additives** | 78.73 | 6.4 | 25.56 | 8.98 | 9.75 |
| **Fly ash** | 273.83 | 110 | 613.73 | – | – |
| **Silica Fume** | – | – | 153.43 | 230 | – |
| **Slag** | 342.29 | – | – | – | – |

**Table 3**
Inventory of conventional construction technology for S1.

| S1 | | | |
|---|---|---|---|
| | Materials | Units | volume |
| **Reinforcing steel** | Reinforcing Steel | t | 151.01 |
| | Galvanised iron wire | kg | 816.39 |
| | Round steel | t | 6.26 |
| | Low alloy steel welding rod | kg | 450.44 |
| | Water | m3 | 11.93 |
| **Concrete** | Concrete | m3 | 1469.76 |
| | Water | m3 | 373.50 |
| | Mortar | m3 | 10.85 |
| | White cement | kg | 7.70 |
| | Hydrated lime | t | 8.37 |
| | Clay | m3 | 39.62 |
| **Formwork** | Reinforcing Steel | kg | 15.15 |
| | Galvanised iron wire | kg | 9.23 |
| | Round Nails | kg | 101.93 |
| | Tie bolts | kg | 666.93 |
| | Iron parts | kg | 50.63 |
| | Cement | t | 0.41 |
| | Sand | m3 | 0.70 |
| | Plate square | m3 | 35.28 |
| | Isolator | kg | 777.54 |
| | Steel support and fittings | kg | 4131.25 |
| | Water | m3 | 0.23 |
| | Composite formwork | m2 | 1952.58 |
| | Wooden supports | m3 | 11.89 |
| **Electricity** | Concrete mixing | kW·h | 487.66 |
| | Formwork making | kW·h | 91.28 |
| | During construction | kW·h | 9688.52 |
| **Transport** | From the supplier to the building site | t·km | 297671.55 |
| | From demolition site to recycling/landfill site | t·km | 722916.63 |
| **Disposal** | Treatment of waste concrete, recycling | t | 3439.11 |
| | Treatment of waste concrete, landfilling | t | 382.12 |

**Table 4**
Life cycle inventory for 3DCP technology for S2–S6.

| | Unit | S2 | S3 | S4 | S5 | S6 |
|---|---|---|---|---|---|---|
| Raw materials | | | | | | |
| Cement | t | – | 607.31 | 970.64 | 1518.28 | 2423.00 |
| Sand | t | 1948.84 | 1224.11 | 679.45 | 1897.85 | 1817.25 |
| Granite | t | – | 1651.13 | – | – | – |
| Water | t | 519.69 | 370.08 | 630.92 | 664.25 | 908.63 |
| Additives | t | 149.42 | 12.15 | 48.51 | 17.04 | 18.50 |
| Fly ash | t | 519.69 | 208.76 | 1164.77 | – | – |
| Silica Fume | t | – | – | – | – | – |
| Slag | t | 649.61 | – | – | – | – |
| Recycled materials | t | 129.92 | 208.76 | 64.07 | 379.57 | 605.76 |
| **Electricity** | | | | | | |
| Power requirements for printing | kW·h | 14311.23 | 14312.23 | 14313.23 | 14314.23 | 14315.23 |
| **Transport** | | | | | | |
| From the supplier to the building site | t·km | 274201.85 | 299761.61 | 269467.94 | 343944.70 | 404120.21 |
| From demolition site to recycling/landfill site | t·km | 665918.78 | 727992.49 | 654422.14 | 835294.27 | 981434.79 |
| **Disposal** | | | | | | |
| Treatment of waste concrete, recycling | t | 3525.46 | 3854.08 | 3464.59 | 4422.15 | 5195.83 |
| Treatment of waste concrete, landfilling | t | 391.72 | 428.23 | 384.95 | 491.35 | 577.31 |

consensus and policy principles regarding time horizons and environmental mechanisms. In addition to global warming potential (GWP), which is a primary focus of this study, we evaluated a suite of midpoint and endpoint impact categories to provide a comprehensive assessment of potential environmental trade-offs associated with integrating waste materials into 3D printed structures. The full set of impact categories considered is presented in Table 5.

## 2.2. Transportation

Transport distances were modeled based on proximity to the construction site, with all raw materials assumed to be sourced from

**Table 5**
List of midpoint impact categories and endpoint impact categories.

| Midpoint impact categories | | | |
|---|---|---|---|
| Impact Category | Unit | Impact Category | Unit |
| Global Warming (GWP) | kg $CO_2$-eq | Terrestrial Ecotoxicity (TET) | kg 1,4-DCB |
| Stratospheric Ozone Depletion (SOD) | kg $CFC_{11}$-eq | Freshwater Ecotoxicity (FEU) | kg 1,4-DCB |
| Ionizing Radiation (IR) | kBq Co-60-eq | Marine Ecotoxicity (MET) | kg 1,4-DCB |
| Ozone Formation, Human Health (OFHH) | kg $NO_x$-eq | Human Carcinogenic Toxicity (HCT) | kg 1,4-DCB |
| Fine Particulate Matter Formation (FPMF) | kg $PM_{2.5}$-eq | Human Non-carcinogenic Toxicity (HNCT) | kg 1,4-DCB |
| Ozone Formation, Terrestrial Ecosystems (OFTE) | kg $NO_x$-eq | Land Use (LU) | $m^2$a crop-eq |
| Terrestrial Acidification (TA) | kg $SO_2$-eq | Mineral Resource Scarcity (MRS) | kg Cu-eq |
| Freshwater Eutrophication (FET) | kg P-eq | Fossil Resource Scarcity (FRS) | kg oil-eq |
| Marine Eutrophication (MEU) | kg N-eq | Water Consumption (WC) | $m^3$ |
| **Endpoint area of protection** | | | |
| Impact Category | | Unit | |
| Human Health | | Daily | |
| Ecosystems | | Species/year | |
| Resources | | USD2013 | |

the nearest supplier. An average transport distance of 70 km was applied, derived from the typical spatial dimensions of the local metropolitan area centered on the construction site.

End-of-life disposal pathways were defined in accordance with the local Metropolitan Area Environmental Sanitation Facilities Special Plan [45]. The scenario assumes 100 % of construction waste is diverted from uncontrolled disposal. Based on policy targets, concrete waste was modeled as 90 % being transported to a recycling facility and 10 % to a sanitary landfill, both located 170 km from the site. These processes occur following the building's assumed 50-year service life.

### 2.3. Calculation of equipment and electricity consumption

The fabrication equipment used in the study for Scenarios 2–6 is assumed to be KUKA KR60 HA robotic arm which is a 6-axis robot arm and has a payload of 30 kg. The printing speed was set to 0.25 m/s, and the motors operated at 50 % of their full capacity (8.4 kW), an operational setup validated for large-scale 3D printing in construction [46]. Samples were printed with a cross-section of 150 mm × 50 mm [47]. Supplementary equipment included a Fangyuan JZC350 self-falling double-cone reverse-discharge concrete mixer (total power: 5.5 kW), used for mixing plastic and semi-dry concrete, and a T0808SD concrete pump with a rated power of 37 kW.

The total active construction time $t$ was calculated as the total concrete volume ($V$) divided by the volumetric printing rate $v$. The total energy consumption for 3DCP fabrication was subsequently calculated as the sum of the energy consumed by each piece of equipment $i$, according to the equation:

$$E_{3D} = \sum_{i=1}^{3} \frac{VW_i}{v} = \sum_{i=1}^{3} W_i t_i, \tag{2}$$

where $V$ is the volume of concrete required for the building, $v$ is the volume of printing that can be achieved per hour, $W$ is the power of the different manufacturing equipment.

### 2.4. Carbonation

Carbonation uptake over the concrete life cycle was quantified using the Lagerblad model, which provides a framework for estimating $CO_2$ offset through atmospheric carbonation [48]. Carbonation rate depends on environmental conditions, concrete strength, and material composition, and this rate typically ranges from 0.5 to 15 mm per year [49]. For instance, carbonation proceeds more rapidly indoors than outdoors and is slower in high strength concrete. In this study, the total carbonation depth over a 50-year service life was estimated for each scenario (S1–S6) by accounting for concrete strength, material properties, and exposure conditions in both interior and exterior environments. Although originally developed for conventionally cast concrete, this modeling approach has been adopted in recent LCA studies of 3D printed concrete [35]. Despite the inherent simplifications, including carbonation provides a more comprehensive representation of life cycle carbon flows than omitting it, as exclusion would systematically overestimate net emissions.

The carbonation depth was modeled according to the classical diffusion-reaction equation:

$$d = k^* \sqrt{t}, \tag{3}$$

where $d$ is the carbonation depth (mm), $k$ is an environmental rate constant (ranging from 1 to 15 mm/year$^{1/2}$ in this study to reflect varying exposure conditions), and $t$ is the time period for carbonation (50 years). The total carbonated volume of concrete ($V_{carbonated}$) was subsequently calculated by integrating the carbonation depth over the total air-exposed surface area ($A$) for each structural element:

$$V_{carbonated} = \sum A^* d. \tag{4}$$

The mass of $CO_2$ sequestered through carbonation was then estimated based on the carbonated volume and the material composition of the concrete. Following established methodology, we assumed that approximately 75 wt% of the calcium oxide (CaO) present in the cement clinker undergoes carbonation, as indicated by phenolphthalein testing [35]. The associated $CO_2$ uptake was calculated as:

$$kgCO_2unptaked = 0.75{*}CaO{*}\frac{MCO_2}{MCaO}\left(\frac{kg}{m^3}\right), \tag{5}$$

where $d$ denotes the carbonation depth, $k$ represents an environmental effect constant (ranging from 1 to 15 in this research), $t$ stands for the carbonation duration in years (set to 50 in this study), $A$ is the air-exposed area, CaO refers to the content of calcium oxide in concrete, $MCO_2$ denotes the molar mass of carbon dioxide, and MCaO represents the molar mass of calcium oxide. This method offers a conservative calculation of the carbonation sink throughout the entire life cycle of concrete.

It is important to clarify the scope of carbonation modeling in this LCA. In this study, $CO_2$ uptake through carbonation is quantified as a negative emission in the life cycle inventory, consistent with established approaches for assessing the carbon footprint of concrete [48,49]. While carbonation can influence long-term durability by lowering the pore solution pH and potentially initiating reinforcement corrosion, such durability effects are not modeled here.

Specifically, this study does not couple the calculated carbonation depth with a service-life or corrosion-propagation model to estimate maintenance needs, damage progression, or potential reductions in service life. Addressing these aspects would require probabilistic frameworks that integrate carbonation kinetics with cover depth, corrosion initiation thresholds, and corrosion propagation. This research direction remains active and complex, but falls beyond the scope of this comparative LCA. To assess the effect of uncertainty in carbonation assumptions, a sensitivity analysis on carbonation depth was conducted, with results discussed in Section 3.3.

Accordingly, the durability implications of carbonation and their potential influence on life cycle environmental outcomes are acknowledged as important topics for future, more integrated assessments.

### *2.5. Treatment of durability-related uncertainty in life cycle assessment*

In building LCA, durability does not directly generate environmental impacts but affects life cycle results through several indirect mechanisms. First, a shorter actual service life increases the environmental burden per functional unit, as the embodied impacts of materials and construction are amortized over a reduced period or necessitate more frequent replacement to deliver the same building function. Second, durability-related performance issues may result in additional maintenance and repair activities during the use phase, leading to extra material, energy, and transportation inputs, which are not explicitly modeled in this study. Third, premature degradation or reduced material integrity at the end of life may affect carbonation uptake and recycling potential, thereby reducing associated environmental credits.

Due to the lack of consistent long-term durability data for emerging 3DCP systems, these pathways are not explicitly quantified in the present model. Instead, a uniform service life assumption is adopted to maintain comparability across scenarios. While the absolute magnitude of environmental impacts may be sensitive to durability performance, the relative ranking among scenarios is expected to be robust, as all scenarios are evaluated under the same conservative lifespan assumption.

Durability-related uncertainties may influence the effective service life of 3D printed and waste-based concrete systems. As service life directly affects processes occurring during the use stage, particularly long-term carbonation uptake, a sensitivity analysis on the degree of carbonation was conducted to explore the potential influence of service-life-related variability on life cycle results.

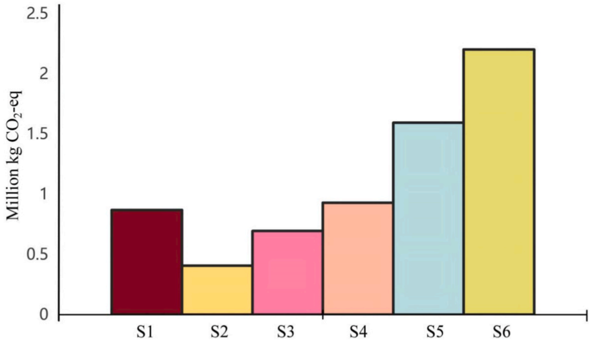


**Fig. 4.** Comparison of $CO_2$ emissions for six scenarios.

## 3. Results

### 3.1. Environmental impact interpretation

Fig. 4 compares the GWP, expressed in carbon dioxide equivalent ($CO_2$-eq), across the six assessed scenarios. The results reveal that the environmental performance of 3DCP is not inherently low-carbon; its life cycle carbon footprint depends critically on material composition and process efficiency.

Scenario 2, which employed a geopolymer binder derived from brick waste, achieved the lowest emissions, a 53.1 % reduction in carbon emissions compared to conventional construction (S1). Scenario 3, incorporating waste glass, also demonstrated a moderate reduction of 20.1 %, and this reduction was primarily attributed to decreased cement consumption.

In contrast, Scenarios 4–6 resulted in higher emissions than the conventional baseline, with the increases being 7.0 %, 83.2 %, and

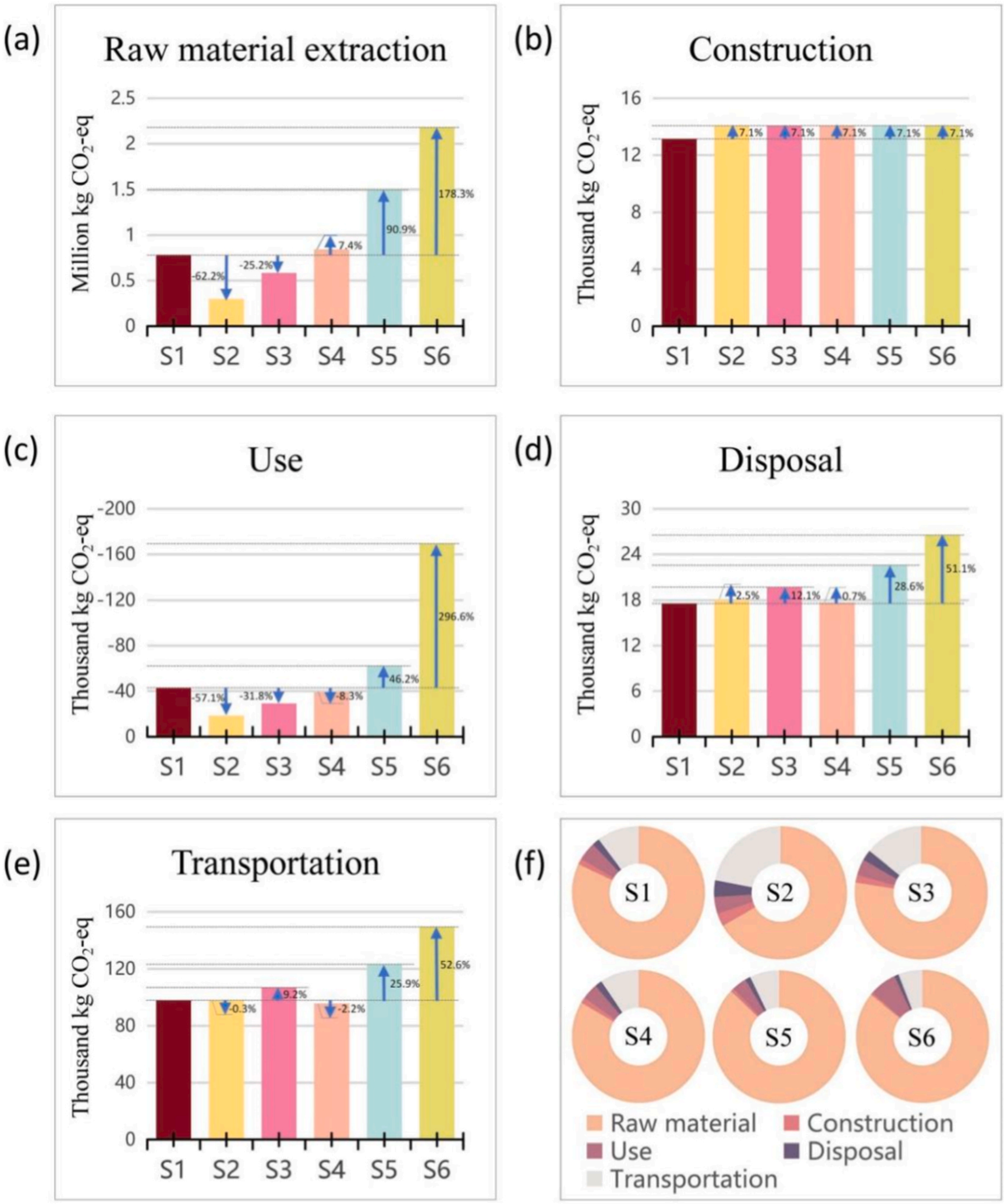


**Fig. 5.** Comparison of $CO_2$ emissions at different stages of scenarios 1–6. (a)–(e) Raw material extraction, construction, use, disposal, and transportation stages emissions; (f) Percentage of $CO_2$ emissions at each stage.

153.2 % respectively. These results demonstrate that the decarbonization potential of 3DCP is conditional and underscore that its climate benefits are only realized through strategic material selection and optimized process design.

Fig. 5 presents a comparative LCA of $CO_2$-equivalent emissions across the six scenarios, evaluating contributions from five distinct phases: raw material extraction, construction, use, disposal, and transportation.

The analysis reveals that the raw material phase dominates the emission profiles across all scenarios, serving as the primary driver of overall carbon footprints. Scenario 2 exhibits the most substantial reduction in emissions during this phase. This result, from effective material substitution, aligns with its lowest total emissions.

Emissions from the construction phase, which includes energy consumption for both conventional pouring and 3D printing processes, exhibit minimal variability across scenarios and represent a relatively small fraction of the total life cycle impact. This indicates limited potential for emission reductions through construction phase optimization alone.

The use phase includes $CO_2$ uptake through concrete carbonation, represented as negative emissions in the figure. Scenario 6 exhibits the highest carbonation potential, a result attributed to its elevated cement content and resulting carbonation capacity, highlighting the influence of material composition on long-term carbon dynamics.

Emissions from the disposal phase, which result from landfilling and recycling processes, were lowest in S1 and S4 due to reduced material consumption and higher recyclability. Transportation emissions varied significantly across scenarios, with S2 and S4 exhibiting the lowest impacts, a benefit attributable to their reduced transport weights.

Critically, Fig. 5(f) visualizes the proportional distribution of emissions across life cycle phases, confirming that raw material extraction and processing represent the largest contributors in all scenarios. The construction phase consistently accounts for the smallest proportion, while transportation-related emissions exhibit notable scenario-dependent variability. These findings underscore that substantial emission reductions in 3DCP depend foremost on low-carbon material design, with secondary gains achievable through optimized logistics and end-of-life management.

Fig. 6 analyzes the principal factors driving carbon dioxide equivalent emissions across the 3DCP scenarios, revealing fundamental differences in their environmental profiles. Cement content emerges as the dominant contributor to greenhouse gas emissions in Scenarios S3–S6, responsible for 73.20 %–97.24 % of life cycle emissions. This finding aligns with prior studies [34,50] and explains the increasing emissions observed from S2 to S6. This trend corresponding directly to rising cement proportions in the mixes. The high embodied carbon of cement production establishes a clear correlation between its usage and the overall environmental impact of building fabrication.

Transportation and chemical additives also represent significant emission sources, contributing 6.78 %–23.95 % and 1.75 %–51.18 % of total impacts, respectively. In Scenario 2, which employs a cement-free geopolymer, additives constitute the primary emission source. This pattern reflects the dual influence of fuel-intensive transport logistics and energy-consuming additive manufacturing processes. The substantial additive demand in 3DCP, necessary to meet printability requirements, further amplifies their relative contribution to the life cycle footprint.

Notably, the analysis also reveals the capacity of 3DCP to enable circularity and carbon uptake. The negative values associated with recycled materials and carbonation represent substantial emission offsets. For instance, the use of waste rubber in S4 offsets 21.75 % of

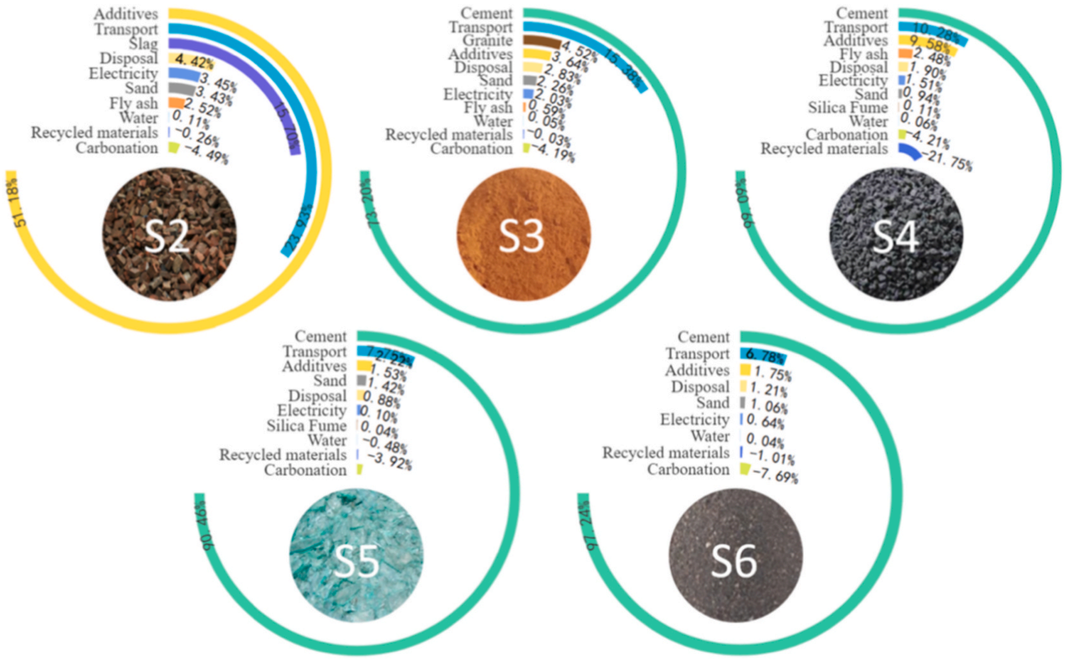


**Fig. 6.** The main factors contributing to $CO_2$ emissions in S2–S6.

greenhouse gas emissions by diverting material from landfills and avoiding virgin resource extraction. Similarly, carbonation resulting from the reaction between atmospheric $CO_2$ and alkaline components in the concrete offsets 3.92 %–7.69 % of total emissions across the scenarios. These mechanisms demonstrate how 3DCP can transform waste into value and incorporate carbon sequestration into the built environment, supporting its potential role in a net-zero construction paradigm.

Fig. 7 presents a comparative LCA across 18 midpoint and three endpoint impact categories, evaluating conventional construction alongside five 3DCP scenarios. The results reveal substantial variations in environmental performance, resource efficiency, and ecosystem health, highlighting both the potential advantages and trade-offs of 3DCP when compared to conventional methods.

Conventional construction demonstrates the highest environmental impact across multiple midpoint categories, notably FEU, FET, MET, HCT, LU, and MRS. These impacts stem primarily from the use of reinforced concrete: steel production consumes substantial fossil energy and mineral resources, emits heavy metals during smelting, requires extensive land for mining and stockpiling, and contributes to resource depletion due to iron ore scarcity.

Scenarios 2 and 3 exhibit markedly reduced environmental footprints. S2, which utilizes a cement-free geopolymer, demonstrates the lowest overall impact, attributable to reduced cement usage, incorporation of recycled materials, and decreased dust emissions. Conversely, S4 to S6 show increasingly adverse environmental impacts, correlating directly with higher cement content and greater material mass.

The sustainability advantage of optimized 3DCP is clearly demonstrated in the endpoint impact results. S2 performs best overall, with the lowest impact on human health, resources, and ecosystem quality. It performs especially well in minimizing human health risks due to lower emissions during construction and use, and shows minimal resource demand through precise material application and waste valorization. In stark contrast, S5 and S6 with high cement and additive usage approach the detrimental impact levels of conventional construction, highlighting that unsustainable material choices can negate the technological benefits of 3DCP.

While these findings illustrate 3DCP's potential for significant multi-dimensional environmental impact reduction, this hinges on the adoption of low-carbon, circular material strategies. Therefore, its sustainability is contingent on informed material selection and process design, underscoring the need for integrated LCA in guiding its development.

### *3.2. Monte Carlo simulation*

The uncertainty in life cycle greenhouse gas emissions for the six scenarios, evaluated via a Monte Carlo simulation, is shown in Fig. 8. To more accurately represent real-world variability than deterministic assessments allow, as the latter rely on single-point estimates, this approach defines key input parameters using probability distributions derived from mean values and standard deviations in the Ecoinvent database [51]. We performed 10,000 iterations per scenario to determine the GWP within a 95 % confidence interval.

A Monte Carlo simulation was applied to the total life cycle impacts of each construction scenario to quantify overall uncertainty, in line with common practice in LCA studies. The resulting uncertainty ranges implicitly capture variability in key modeling assumptions, including transportation processes and material substitution ratios. This approach to uncertainty analysis has been widely adopted in previous LCA research [52–54].

The results demonstrate symmetric distributions characterized by minimal divergence between mean and median values, low standard errors, and limited influence from extreme values. These metrics collectively indicate a robust central tendency and low uncertainty in the emission estimates. The consistent observation of a slight right-skew across distributions further suggests that the

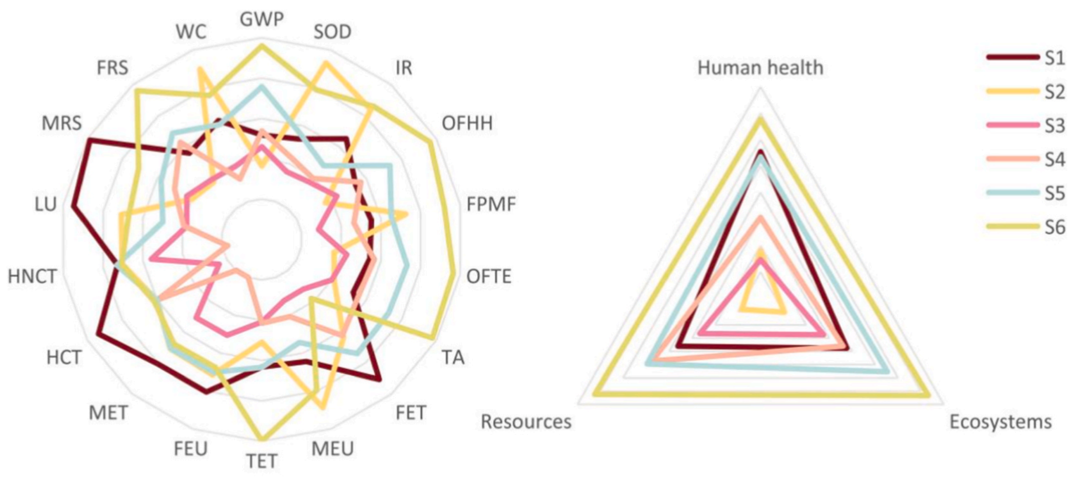


(a) 18 midpoint impact categories (b) 3 endpoint impact categories

**Fig. 7.** Environmental impact indicators of 3DCP and conventional construction processes in six scenarios. (a) Midpoint impact; (b) Endpoint impact. Abbreviations are defined in Table 4.

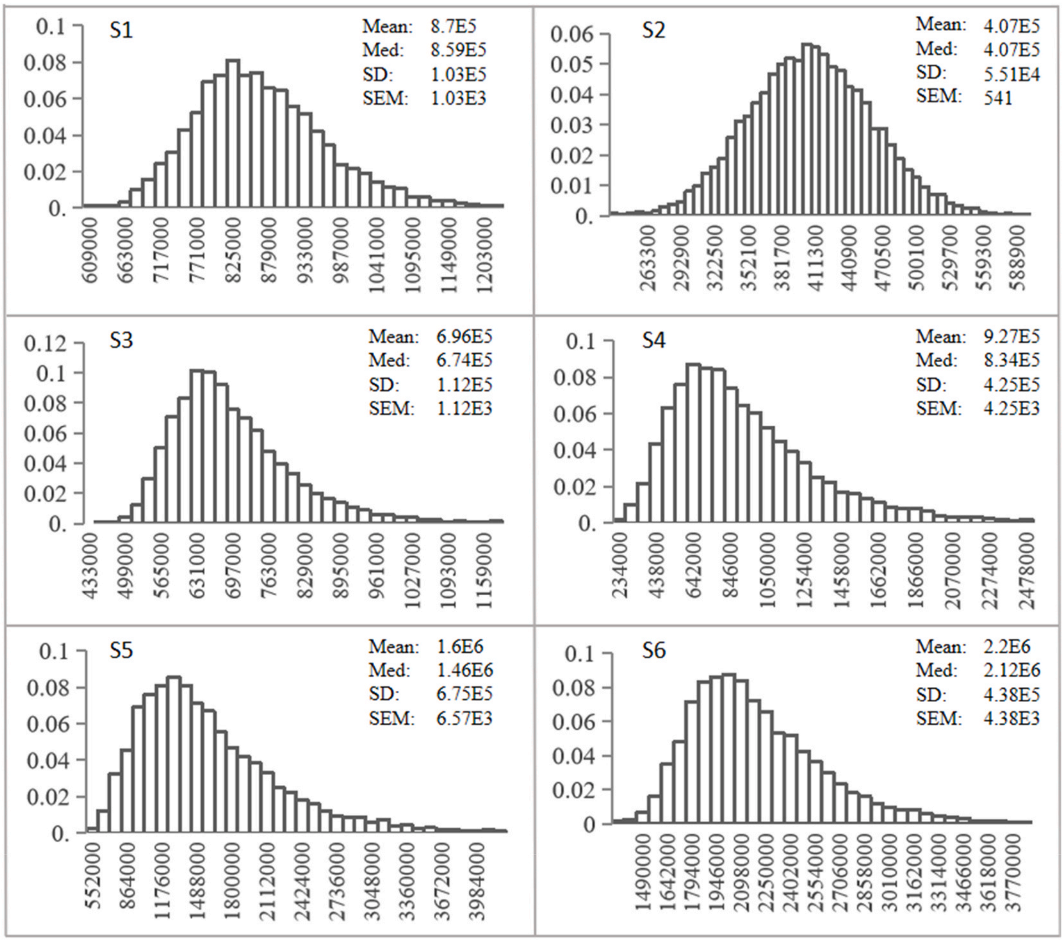


**Fig. 8.** Uncertainty analysis for six scenarios.

median provides a more representative estimate of expected emissions than the mean. Consequently, the narrow spread of results confirms that the greenhouse gas emissions for each scenario exhibit high repeatability and are unlikely to fluctuate significantly due to stochastic variations in input parameters.

### *3.3. Sensitivity analysis on key parameters*

To evaluate the robustness of the key findings and quantify the influence of critical input parameters, a comprehensive sensitivity analysis was conducted. Four parameters with high contributions to total impacts or notable practical uncertainty were selected: cement content, additive dosage, transport distance, and degree of carbonation. Recycled material quality was not treated as an independent variable but was represented indirectly through variations in achievable cement substitution levels and additive dosages, reflecting practical constraints associated with the performance of waste-derived materials. Each parameter was independently varied by ±20 % from its baseline value while all others were held constant. The resulting changes in GWP for each scenario were computed and expressed as percentage deviations from the base-case results. The outcomes are presented in Fig. 9.

Cement content is the dominant sensitivity factor across all mix designs. As expected, scenarios S3–S6, which rely heavily on OPC, exhibit the strongest response: a ±20 % change in cement content leads to roughly ±15–20 % variation in GWP. This underscores the central importance of reducing cement content for decarbonizing 3DCP.

Additive dosage is also a major driver, particularly for optimized mixes. In scenario S2, which uses a cement-free binder, additive dosage is the most influential parameter, with a ±20 % change resulting in a ±10.2 % variation in GWP. This reflects a key trade-off: while additives are essential for achieving printability, they carry substantial environmental burdens. Optimizing both the type and amount of additives is therefore critical for improving the sustainability of low-clinker or clinker-free 3DCP formulations.

Transport distance shows moderate sensitivity. Although the directional effect is consistent across all scenarios, the magnitude of sensitivity varies from approximately ±1.4 % to ±4.8 % for a ±20 % change. Scenarios involving heavier materials or longer sourcing distances show greater sensitivity, indicating that localized sourcing and logistics optimization can yield meaningful, though secondary, emissions reductions.

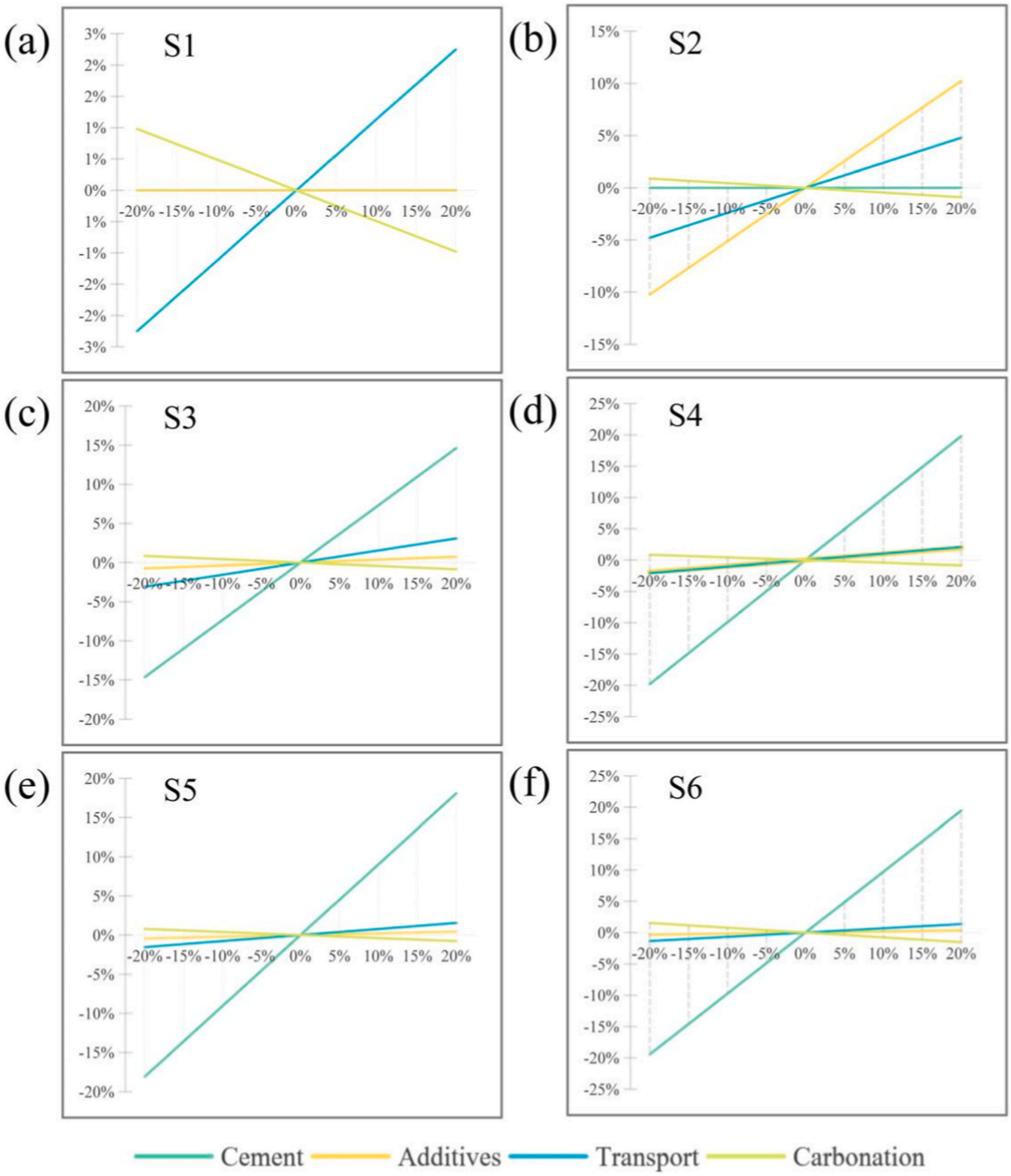


**Fig. 9.** Sensitivity of GWP to variations (±20 %) in key input parameters.

Carbonation provides a modest beneficial offset. Changes in the assumed degree of carbonation produce symmetric but negative GWP responses for cement-containing scenarios: a 20 % increase in carbonation rate lowers GWP by 0.8–1.5 %. While this supports carbonation as a credible carbon sink, its influence is an order of magnitude smaller than that of cement content within plausible parameter ranges. The results suggest that uncertainties in carbonation modeling, such as exposure conditions and carbonation rates, exert a limited influence on total life cycle impacts and do not change the relative ranking of scenarios.

With respect to overall robustness, the comparative ranking of scenarios remains unchanged across the full sensitivity analysis. Scenario S2 consistently exhibits the lowest GWP, whereas S5 and S6 retain the highest impacts. The substantial 53 % reduction achieved by S2 relative to S1 remains stable, with deviations of less than ±2 percentage points across all parameter variations. These results confirm the robustness of the central conclusion, which holds that 3DCP delivers significant life cycle carbon savings only when paired with low-carbon, circular material strategies. This conclusion is not dependent on specific parameter choices.

## 4. Discussion

Through a multi-scenario LCA, this study provides a systematic evaluation of the environmental performance and operational boundaries of 3DCP. The results demonstrate that the sustainability of 3DCP is not intrinsic but is instead contingent upon specific material formulations and process design. Optimized systems, leveraging precise material control and the integration of waste streams, can achieve significant reductions in environmental impact, establishing a scalable low-carbon construction method. However, ill-conceived material selection can diminish these benefits, underscoring the imperative for context-specific implementation strategies. Although absolute impact values vary under Monte Carlo simulation, the relative ranking of scenarios remains robust across plausible ranges of transportation distances, additive dosages, and achievable cement substitution levels associated with recycled material quality.

These findings align directly with the strategic pillars of the GCCA 2050 Net-Zero Roadmap. Our results substantiate key decarbonization pathways advocated by the roadmap, particularly through cement substitution, material efficiency, and enhanced carbonation. For example, Scenario 2 that employs a cement-free geopolymer demonstrates the potential to surpass the GCCA's 2030 target of a 25 % reduction in $CO_2$ emissions per cubic meter of concrete. Furthermore, the identification of risk factors in underperforming scenarios (S4–S6) provides actionable insights for mitigating unintended emissions during the implementation of emerging technologies.

### *4.1. A multidimensional pathway to decarbonization*

To align 3DCP with global climate targets, we propose an integrated strategy spanning materials, processes, and policies.

- Material System Innovation: Accelerate the development of low-clinker binders using reactive waste materials (e.g., brick, slag, ash) to meet cement substitution targets. Foster mix designs that synergize waste incorporation with enhanced carbonation, directly contributing to the GCCA's goals of 9 % emission reduction from cement and binders and 6 % from concrete carbonation.
- Process and Energy Optimization: Deploy digital tools like AI and digital twins to optimize printing parameters, structural efficiency, and energy consumption, supporting the roadmap's 22 % reduction target from design and construction efficiency. Decarbonize printing operations by powering equipment with renewable energy and implementing waste-heat recovery, advancing the 5 % emissions reduction target from electricity and heat.
- Policy and Standardization: Establish regulatory and market incentives to promote sustainable 3DCP. Update building standards to mandate material provenance, carbon transparency, and waste integration. Implement carbon-aware public procurement and fiscal policies to accelerate industry-wide adoption of circular, low-carbon 3DCP technologies.

By implementing these aligned actions, 3DCP can transition from a novel prototyping technique into a pillar of sustainable, equitable, and climate-resilient construction.

### *4.2. Trade-offs and practical constraints of 3DCP*

While optimized 3DCP scenarios demonstrate substantial potential for life cycle carbon reduction, several trade-offs and practical constraints must be considered. First, many 3DCP formulations require elevated cement or binder contents to achieve adequate buildability and early-age strength. As demonstrated by scenarios S4–S6, such material intensification can offset or even outweigh the environmental benefits associated with automated construction, leading to higher overall emissions than conventional casting.

The environmental performance of 3DCP is also strongly influenced by its reliance on chemical admixtures. High dosages of rheology modifiers and superplasticizers, while essential for printability and interlayer stability, contribute disproportionately high embodied emissions. This introduces a trade-off between optimizing fresh-state performance and minimizing life cycle environmental impacts, particularly in low-clinker or cement-free formulations.

Construction-stage energy demand adds further variability. Although the absolute contribution of printing energy is generally secondary to cement production, its relative significance increases in regions with carbon-intensive electricity grids or energy-inefficient printing systems. Accordingly, decarbonizing energy supply and improving process efficiency are necessary complements to material-level optimization.

Taken together, these trade-offs indicate that the environmental benefits of 3DCP are not inherent to the technology itself but depend on coordinated optimization of material composition, admixture strategy, and energy provision.

### *4.3. Limitations and future research directions*

Notwithstanding its contributions, this study has several limitations that suggest productive avenues for future research.

Equivalence among construction scenarios is defined at the level of functional structural performance, rather than through detailed structural design optimization or a full probabilistic assessment of mechanical anisotropy. Although the 3DCP mixtures considered were sourced from peer-reviewed studies in which printability and mechanical performance were experimentally validated, the layer-wise fabrication inherent to 3D printing introduces anisotropic mechanical behavior, particularly across interlayer regions. Variations in anisotropy-aware structural design, reinforcement strategies, and print orientation can affect material demand, safety margins, and long-term performance in practical applications. These factors were not explicitly modeled and thus constitute an important source of uncertainty.

While this study evaluated several prominent waste streams as supplementary cementitious materials, it did not encompass the full range of potential recycled or bio-based alternatives. Expanding material portfolios to include a wider array of industrial by-products, agricultural wastes, or locally sourced materials could further enhance the circular economy potential of 3DCP and warrants further investigation.

Carbonation uptake was modeled using simplified assumptions regarding exposure conditions and carbonation rates. Although carbonation can contribute to net carbon reduction, especially during the use and end-of-life phases, the adopted model does not explicitly account for potential differences in carbonation behavior arising from layered microstructures and interfacial porosity in 3D printed elements. Accordingly, the carbonation results should be interpreted as indicative rather than predictive, and future studies integrating microstructural characterization with carbonation modeling would enhance accuracy.

A uniform service life of 50 years was assumed for all scenarios to ensure a transparent and comparable cradle-to-grave assessment. While this assumption aligns with common practice in building LCA studies, it does not capture potential differences in durability among 3DCP systems, particularly those incorporating waste-derived materials. Factors such as interlayer porosity, shrinkage behavior, moisture transport, and the long-term stability of recycled constituents may influence degradation mechanisms and maintenance requirements. If the actual service life of certain 3DCP systems is shorter than assumed, the environmental benefits identified here could be partially reduced. Nevertheless, because the same service life assumption was applied consistently across all scenarios, the relative ranking of scenarios is unlikely to change.

### *4.4. Implications for global applicability and regional contexts*

Although this study is based on data from China, providing a concrete case analysis, its framework and findings offer valuable insights for global applications. The core conclusion holds that the sustainability of 3DCP depends on material innovation and the integration of circular economy principles, and this conclusion remains broadly applicable. However, the magnitude of benefits and optimal implementation pathways may vary regionally due to contextual factors.

The carbon intensity of the local electricity grid directly affects the impacts of material production and 3D printing operations. In regions with a higher share of renewable energy, such as Europe, the use phase contributes less to the total carbon footprint, making material-related impacts more prominent. Conversely, in areas reliant on coal, decarbonizing energy supply becomes a prerequisite alongside material innovation to achieve net-zero goals.

Geographic distribution of material suppliers, construction sites, and recycling facilities also influences transport burdens. Regions with efficient rail or waterway logistics, or those promoting localized material cycles, can substantially reduce transport emissions. While our sensitivity analysis shows transport as a moderate contributor, its importance rises in regions with long or inefficient supply chains.

The environmental credit in our model depends on avoided landfill burdens. In regions with high landfill taxes, advanced recycling infrastructure, or strict landfill bans, the baseline disposal impact differs. Although the absolute carbon offset from using waste may be smaller in such contexts, stronger economic incentives and regulatory drivers could accelerate adoption of circular strategies.

For global applicability, the quantitative results should be recalibrated using regional life cycle inventory data. Nevertheless, the strategic hierarchy remains consistent: reducing cement content is universally paramount; optimizing logistics is broadly beneficial; and integrating waste streams is most impactful where landfill diversion offers significant environmental savings. Policymakers and practitioners can apply the framework developed here, supplemented with local data, to identify the most effective decarbonization levers for 3DCP in their specific contexts.

Importantly, regional differences are expected to influence primarily the absolute magnitude of life cycle impacts rather than the relative ranking of construction scenarios. Variations in electricity grid carbon intensity and waste management practices may affect the contribution of energy- and waste-related processes, but they do not fundamentally change the dominant role of cement content in driving overall emissions. Consequently, scenarios employing low-clinker or cement-free materials are expected to remain environmentally preferable across regions, whereas scenarios with high cement demand would continue to exhibit higher impacts. Only in regions where electricity supply is fully decarbonized and landfill disposal is largely eliminated would the relative contributions of waste offset and construction-stage energy be substantially reduced, although the comparative advantage of material-efficient scenarios would persist.

## 5. Conclusion

This study employed a comprehensive LCA to evaluate the environmental performance of 3DCP against conventional construction methods across multiple impact categories. Focusing on greenhouse gas emissions and other key indicators under varying material scenarios, the analysis contextualizes results can help realizing the GCCA 2050 Net-Zero Roadmap framework.

Findings reveal that the environmental benefits of 3DCP are conditional rather than inherent, depending critically on material formulation and process design. Scenario 2 that features low-cement composition and optimized printing achieved substantially lower greenhouse gas emissions than conventional construction. In this scenario, waste material integration offset 21.75 % of carbon emissions by avoiding virgin material production, while concrete carbonation contributed an additional 3.92 %–7.69 % reduction in the total carbon footprint. Conversely, Scenarios S4–S6, which used high cement and additive content, resulted in higher emissions than conventional construction, underscoring the risks of poor material selection.

Cement was identified as the dominant contributor to greenhouse gas emissions across most 3DCP scenarios, with transportation and chemical additives representing secondary yet substantial sources. The rebar-free nature of many 3DCP structures and their capacity to incorporate recycled materials align closely with GCCA roadmap priorities, including cement substitution and clinker-related energy savings.

The robustness of these findings was confirmed through a multi-parameter sensitivity analysis. Cement content emerged as the dominant driver of life cycle emissions, while additive dosage was particularly influential for low-clinker mixes. Crucially, the relative environmental performance ranking of all scenarios remained unchanged across ±20 % variations in key input parameters. This demonstrates that the conclusion is robust to reasonable parameter uncertainties. The conclusion is that substantial carbon reductions are achievable only through optimized, waste-valorized 3DCP.

To realize the full sustainable potential of 3DCP, we propose three integrated strategies: 1) Material innovation: Develop advanced formulations that enhance both waste material integration and carbonation potential, supporting roadmap targets for cement substitution and $CO_2$ uptake. 2) Process optimization: Implement digital twins and artificial intelligence to optimize printing parameters, energy efficiency, and structural design, while accelerating transition to renewable energy sources. 3) Policy integration: Establish standardized sustainability indicators requiring disclosure of carbon emissions and recycled content, supported by fiscal incentives that prioritize low-carbon, circular material flows. Through these coordinated efforts, 3DCP can transition from a promising technology to a cornerstone of sustainable construction, supporting the industry's transition toward net-zero emissions.

## CRediT authorship contribution statement

**Xiaoshao Mu:** Writing – original draft, Methodology, Investigation, Formal analysis, Conceptualization. **Xiaoling Zhang:** Writing – review & editing, Methodology, Formal analysis. **Gang He:** Writing – review & editing, Investigation. **K.M. Liew:** Writing – review & editing, Supervision, Resources, Methodology, Investigation, Funding acquisition, Conceptualization.

## Declaration of competing interest

The authors declare that they have no known competing financial interests or personal relationships that could have appeared to influence the work reported in this paper.

## Acknowledgments

The authors acknowledge the supports provided by the Research Grants Council of the Hong Kong Special Administrative Region, China (Project No. 8780054, STG5/E-103/24-R). The authors would like to express their sincere gratitude to Mr. Guo Feifan from Central China Real Estate Group for providing the original data on materials required for the construction project as well as relevant technical support.

## Data availability

No data was used for the research described in the article.

## References

[1] P. Dashti, S. Ranjbar, S. Ghafari, A. Ramezani, F.M. Nejad, RSM-based and environmental assessment of eco-friendly geopolymer mortars containing recycled waste tire constituents, J. Clean. Prod, 428 139365 (2023), https://doi.org/10.1016/j.jclepro.2023.139365.
[2] S. Singh, M.M. Dalbehera, S. Maiti, R.S. Bisht, N.B. Balam, S.K. Panigrahi, Investigation of agro-forestry and construction demolition wastes in alkali-activated fly ash bricks as sustainable building materials, Waste Manag. 159 (2023) 114–124, https://doi.org/10.1016/j.wasman.2023.01.031.
[3] A. Katebi, H. Soleymani Tushmanlo, G. Asadollahfardi, Environmental life cycle assessment and economic comparison of different roof systems, J. Build. Eng. 76 (2023) 107316, https://doi.org/10.1016/j.jobe.2023.107316.
[4] N.J. Gonsalves, A. Yusuf, O. Ogunseiju, A. Akanmu, Evaluation of concrete workers' interaction with a passive back-support exoskeleton, Eng. Constr. Archit. Manag. 31 (2023) 4585–4601, https://doi.org/10.1108/ECAM-12-2022-1156.
[5] Md, A. Uddin, M. Shahabuddin, M. Jameel, M. Rahman, Md.A. Hosen, F. Alanazi, M. AbdelMongy, M.S. El-kady, sustainable construction practices in urban areas: innovative materials, technologies, and policies to address environmental challenges, Energy Build. 341 (2025) 115831, https://doi.org/10.1016/j.enbuild.2025.115831.
[6] M.H. Raza, E. Kravchenko, S. Besklubova, G. Lazorenko, M. Markelov, A. Kasprzhitskii, R.Y. Zhong, 3D printing of recycled materials for sustainable construction: a comprehensive economic and life cycle assessment, Renew, Sustain. Energy Rev 223 (2025) 116059, https://doi.org/10.1016/j.rser.2025.116059.
[7] L.I.C. Fernandez, L.R. Caldas, O.A. Mendoza Reales, Environmental evaluation of 3D printed concrete walls considering the life cycle perspective in the context of social housing, J. Build. Eng. 74 (2023) 106915, https://doi.org/10.1016/j.jobe.2023.106915.
[8] Q. Shahzad, M. Umair, S. Waqar, Bibliographic analysis on 3D printing in the building and construction industry: printing systems, material properties, challenges, and future trends, J. Sustain. Constr. Mater. Technol 7 (2022) 198–220, https://doi.org/10.47481/jscmt.1143239.
[9] H. Yu, W. Zhang, J.X. Liew, B. Yin, K.M. Liew, Simulating material flow and extrusion dynamics in 3D concrete printing, Comput. Methods Appl. Mech. Eng. 449 (2026) 118575, https://doi.org/10.1016/j.cma.2025.118575.
[10] H. Yu, W. Zhang, B. Yin, W. Sun, A. Akbar, Y. Zhang, K.M. Liew, Modeling extrusion process and layer deformation in 3D concrete printing via smoothed particle hydrodynamics, Comput. Methods Appl. Mech. Eng. 420 (2024) 116761, https://doi.org/10.1016/j.cma.2024.116761.
[11] C. Buchanan, L. Gardner, Metal 3D printing in construction: a review of methods, research, applications, opportunities and challenges, eng, Struct 180 (2019) 332–348, https://doi.org/10.1016/j.engstruct.2018.11.045.
[12] A. Habibi, R. Buswell, M. Osmani, M. Aziminezhad, Sustainability principles in 3D concrete printing: analysing trends, classifying strategies, and future directions, J. Build. Eng. 98 (2024) 111354, https://doi.org/10.1016/j.jobe.2024.111354.

[13] M.T. Souza, I.M. Ferreira, E. Guzi de Moraes, L. Senff, A.P. Novaes de Oliveira, 3D printed concrete for large-scale buildings: an overview of rheology, printing parameters, chemical admixtures, reinforcements, and economic and environmental prospects, J. Build. Eng. 32 (2020) 101833, https://doi.org/10.1016/j.jobe.2020.101833.
[14] J. Chung, G. Lee, J.-H. Kim, Framework for technical specifications of 3D concrete printers, Autom. ConStruct. 127 (2021) 103732, https://doi.org/10.1016/j.autcon.2021.103732.
[15] M.P. Tinoco, É.M. de Mendonça, L.I.C. Fernandez, L.R. Caldas, O.A.M. Reales, R.D. Toledo Filho, Life cycle assessment (LCA) and environmental sustainability of cementitious materials for 3D concrete printing: a systematic literature review, J. Build. Eng. 52 (2022) 104456, https://doi.org/10.1016/j.jobe.2022.104456.
[16] A. van Stijn, V. Gruis, Towards a circular built environmentAn integral design tool for circular building components, smart sustain, Built. Environ. 9 (2020) 635–653, https://doi.org/10.1108/SASBE-05-2019-0063.
[17] H. Desing, D. Brunner, F. Takacs, S. Nahrath, K. Frankenberger, R. Hischier, A circular economy within the planetary boundaries: towards a resource-based, systemic approach,, Resour. Conserv. Recycl. 155 (2020) 104673, https://doi.org/10.1016/j.resconrec.2019.104673.
[18] S.S. Mousavi, M. Dehestani, On the possibility of using waste disposable gloves as recycled fibers in sustainable 3D concrete printing using different additives, Sci. Rep. 13 (2023) 10812, https://doi.org/10.1038/s41598-023-37803-9.
[19] S.A. Khan, H. İlcan, E. Aminipour, O. Şahin, A. Al Rashid, M. Şahmaran, M. Koç, Buildability analysis on effect of structural design in 3D concrete printing (3DCP): an experimental and numerical study, Case Stud. Constr. Mater. 19 (2023) e02295, https://doi.org/10.1016/j.cscm.2023.e02295.
[20] M. Lu, W. Ge, Y. Xia, C. Sun, X. Lin, D.C.W. Tsang, T.-C. Ling, Y. Hu, L. Wang, J. Yan, Upcycling MSWI fly ash into green binders via flue gas-enhanced wet carbonation, J. Clean. Prod. 440 (2024) 141013, https://doi.org/10.1016/j.jclepro.2024.141013.
[21] N.G. Akhimien, E. Latif, S.S. Hou, Application of circular economy principles in buildings: a systematic review, J. Build. Eng. 38 (2021) 102041, https://doi.org/10.1016/j.jobe.2020.102041.
[22] G. Bai, L. Wang, G. Ma, J. Sanjayan, M. Bai, 3D printing eco-friendly concrete containing under-utilised and waste solids as aggregates, Cem. Concr. Compos. 120 (2021) 104037, https://doi.org/10.1016/j.cemconcomp.2021.104037.
[23] N.C. Demiral, M. Ozkan Ekinci, O. Sahin, H. Ilcan, A. Kul, G. Yildirim, M. Sahmaran, Mechanical anisotropy evaluation and bonding properties of 3D-printable construction and demolition waste-based geopolymer mortars, Cem. Concr. Compos. 134 (2022) 104814, https://doi.org/10.1016/j.cemconcomp.2022.104814.
[24] K. Shen, T. Ding, C. Cai, J. Xiao, X. Xiao, W. Liang, Feasibility analysis of 3D printed concrete with sludge incineration slag: mechanical properties and environmental impacts, Constr. Build. Mater. 449 (2024) 138521, https://doi.org/10.1016/j.conbuildmat.2024.138521.
[25] M. Colyn, G. van Zijl, A.J. Babafemi, Fresh and strength properties of 3D printable concrete mixtures utilising a high volume of sustainable alternative binders, Constr. Build. Mater. 419 (2024) 135474, https://doi.org/10.1016/j.conbuildmat.2024.135474.
[26] T. Ding, K. Shen, C. Cai, J. Xiao, X. Xiao, W. Liang, 3D printed concrete with sewage sludge ash: fresh and hardened properties, Cem. Concr. Compos. 148 (2024) 105475, https://doi.org/10.1016/j.cemconcomp.2024.105475.
[27] International Organization for Standardization, ISO 14040: Environmental Management — Life Cycle Assessment — Principles and Framework, 2006. Second Ed.
[28] International Organization for Standardization, ISO 14044: Environmental Management — Life Cycle Assessment — Requirements and Guidelines, 2006. First Ed.
[29] D.O. Oyejobi, A.A. Firoozi, D.B. Fernández, S. Avudaiappan, Integrating circular economy principles into concrete technology: enhancing sustainability through industrial waste utilization, Results Eng. 24 (2024) 102846, https://doi.org/10.1016/j.rineng.2024.102846.
[30] L. Wang, Z. Tian, G. Ma, M. Zhang, Interlayer bonding improvement of 3D printed concrete with polymer modified mortar: experiments and molecular dynamics studies, Cem. Concr. Compos. 110 (2020) 103571, https://doi.org/10.1016/j.cemconcomp.2020.103571.
[31] L. Pham, G. Lu, P. Tran, Influences of printing pattern on mechanical performance of three-dimensional-printed fiber-reinforced concrete, 3D print. Addit, Man (Lond.) 9 (2022) 46–63, https://doi.org/10.1089/3dp.2020.0172.
[32] Y. Ding, X. Ou, H. Qi, G. Xiong, T. Nishiwaki, Y. Liu, J. Liu, Interlayer bonding performance of 3D printed engineered cementitious composites (ECC): rheological regulation and fiber hybridization, Cem. Concr. Compos. 154 (2024) 105805, https://doi.org/10.1016/j.cemconcomp.2024.105805.
[33] P.S. Ambily, S.K. Kaliyavaradhan, N. Rajendran, Top challenges to widespread 3D concrete printing (3DCP) adoption – a review, Eur. J. Environ. Civil Eng. 28 (2024) 300–328, https://doi.org/10.1080/19648189.2023.2213294.
[34] I. Muñoz, J. Alonso-Madrid, M. Menéndez-Muñiz, M. Uhart, J. Canou, C. Martin, M. Fabritius, L. Calvo, L. Poudelet, R. Cardona, Life cycle assessment of integrated additive–subtractive concrete 3D printing, Int. J. Adv. Manuf. Technol. 112 (2021) 2149–2159, https://doi.org/10.1007/s00170-020-06487-0.
[35] S. Gislason, S. Bruhn, L. Breseghello, B. Sen, G. Liu, R. Naboni, Porous 3D printed concrete beams show an environmental promise: a cradle-to-grave comparative life cycle assessment, Clean Technol. Environ. Policy 24 (2022) 2639–2654, https://doi.org/10.1007/s10098-022-02343-9.
[36] K. Wang, T. He, W. Xiao, R. Yang, Projections of future spatiotemporal urban 3D expansion in China under shared socioeconomic pathways, landsc, Urban Plan 247 (2024) 105043, https://doi.org/10.1016/j.landurbplan.2024.105043.
[37] H. Zhang, X. Liu, J. Xiao, G. Ji, S. Zhang, S.-C. Hsu, C.-S. Poon, Comparative eco-efficiency assessment of 3D-printed recycled aggregate concrete structure for mid-rise residential buildings, J. Build. Eng. 95 (2024) 110349, https://doi.org/10.1016/j.jobe.2024.110349.
[38] D. of S.Q, Ministry of Construction of the People'S Republic of China, National Unified Compilation Manual for Construction Engineering Basic Quotas, Heilongjiang Science &Technology Press, 1997.
[39] K. Pasupathy, S. Ramakrishnan, J. Sanjayan, 3D concrete printing of eco-friendly geopolymer containing brick waste, Cem. Concr. Compos. 138 (2023) 104943, https://doi.org/10.1016/j.cemconcomp.2023.104943.
[40] W.C. Tang, Z. Wang, Y. Liu, H.Z. Cui, Influence of red mud on fresh and hardened properties of self-compacting concrete, Constr. Build. Mater. 178 (2018) 288–300, https://doi.org/10.1016/j.conbuildmat.2018.05.171.
[41] J. Sun, Y. Zhang, Q. Wu, Y. Wang, H. Liu, H. Zhao, W. Cui, W. Zhang, X. Wang, 3D printed concrete incorporating waste rubber: anisotropic properties and environmental impact analysis, J. Mater. Res. Technol. 33 (2024) 2773–2784, https://doi.org/10.1016/j.jmrt.2024.09.190.
[42] Y. Zhou, H. Luo, K. Anand, A. Singh, Y.M. Xie, Sustainable use of ultrafine recycled glass in additive manufactured (3D printed) reactive powder concrete, Constr. Build. Mater. 419 (2024) 135556, https://doi.org/10.1016/j.conbuildmat.2024.135556.
[43] ReCiPe, A harmonised life cycle impact assessment method at midpoint and endpoint level | the international journal of life cycle assessment, n.d. https://link.springer.com/article/10.1007/s11367-016-1246-y, 2016. (Accessed 7 September 2025).
[44] ReCiPe, A harmonized life cycle impact assessment method at midpoint and endpoint level report I: characterization. https://rivm.openrepository.com/entities/publication/3d19272d-3ee1-4d95-bbc7-3ad21f0a769e, 2016. (Accessed 7 September 2025).
[45] Zhengzhou Metropolitan Area Environmental Sanitation Facilities Special Planning(2017-2035), n.d, https://zrzyhghj.zhengzhou.gov.cn/szjc/3474361.jhtml. (Accessed 7 June 2025).
[46] H. Alhumayani, M. Gomaa, V. Soebarto, W. Jabi, Environmental assessment of large-scale 3D printing in construction: a comparative study between cob and concrete, J. Clean. Prod. 270 (2020) 122463, https://doi.org/10.1016/j.jclepro.2020.122463.
[47] R. Schack, M. Krause, M. Näther, V.N. Nerella, CONPrint3D: 3D-concrete-printing as an alternative for masonry, Bauingenieur 92 (2017) 355–363.
[48] B. Lagerblad, Carbon Dioxide Uptake During Concrete Life Cycle: State of the Art, Swedish Cement and Concrete Research Institute Stockholm, 2005.
[49] C. Pade, M. Guimaraes, The CO2 uptake of concrete in a 100 year perspective, cem, Concr. Res. 37 (2007) 1348–1356, https://doi.org/10.1016/j.cemconres.2007.06.009.
[50] Y. Weng, M. Li, S. Ruan, T.N. Wong, M.J. Tan, K.L. Ow Yeong, S. Qian, Comparative economic, environmental and productivity assessment of a concrete bathroom unit fabricated through 3D printing and a precast approach, J. Clean. Prod. 261 (2020) 121245, https://doi.org/10.1016/j.jclepro.2020.121245.
[51] Quantification of uncertainty in product stage embodied carbon calculations for buildings, Energy Build. 251 (2021) 111340, https://doi.org/10.1016/j.enbuild.2021.111340.

[52] Y. Liu, J. Zhang, J. Xu, Y. Wang, B. Li, S. Zhang, Carbon emission-based life cycle assessment of rural residential buildings constructed with engineering bamboo: a case study in China, J. Build. Eng. 76 (2023) 107182, https://doi.org/10.1016/j.jobe.2023.107182.
[53] L. Xin, S. Li, E.R. Rene, X. Lun, P. Zhang, W. Ma, Prediction of carbon emissions peak and carbon neutrality based on life cycle CO2 emissions in megacity building sector: dynamic scenario simulations of Beijing, Environ. Res. 238 (2023) 117160, https://doi.org/10.1016/j.envres.2023.117160.
[54] J. Li, Y. Wang, C. Xu, S. Liu, J. Dai, K. Lan, Bioplastic derived from corn stover: life cycle assessment and artificial intelligence-based analysis of uncertainty and variability, Sci. Total Environ. 946 (2024) 174349, https://doi.org/10.1016/j.scitotenv.2024.174349.